Available online at www.sciencedirect.com
ScienceDirect
Chinese Journal of Natural Medicines 2019, **17**(12): 0963–0969
Chinese Journal of Natural Medicines

Enantiomeric pairs of meroterpenoids from *Rhododendron fastigiatum*

HUANG Guang-Hui[1], LEI Chun[1*], ZHU Ke-Xin[2], LI Jing-Ya[2], LI Jia[2], HOU Ai-Jun[1*]

[1]*School of Pharmacy, State Key Laboratory of Medical Neurobiology, Fudan University, Shanghai 201203, China;*
[2]*National Center for Drug Screening, State Key Laboratory of Drug Research, Shanghai Institute of Materia Medica, Chinese Academy of Sciences, Shanghai 201203, China*

Available online 20 Dec., 2019

[ABSTRACT] Five pairs of optically pure meroterpenoid enantiomers (**1a/1b**–**5a/5b**) and two known compounds (**6** and **7**) were isolated from *Rhododendron fastigiatum*. Compounds **1a/1b**–**5a/5b** were resolved from naturally scalemic mixtures by chiral HPLC. Their structures were elucidated by spectroscopic methods, X-ray crystallographic experiments, and ECD analyses. Compounds **1a/1b**, **2a/2b**, **3b**, **4a/4b**, and **5a/5b** were new meroterpenoids with different polycyclic systems. Two enantiomeric pairs (**2a/2b** and **3a/3b**), **6**, and **7** exhibited inhibitory effects on protein tyrosine phosphatase 1B (PTP1B) *in vitro*.

[KEY WORDS] *Rhododendron fastigiatum*; Meroterpenoid enantiomers; Protein tyrosine phosphatase 1B

[CLC Number] R284 **[Document code]** A **[Article ID]** 2095-6975(2019)12-0963-07

Introduction

The resource of the *Rhododendron* genus is abundant in China. There are approximately 571 species mainly distributed in South and Southwest China [1]. In addition to the characteristic grayanane diterpenoids from this genus [2–4], the *Rhododendron* meroterpenoids have also triggered attentions in the field of natural products. These metabolites not only possess diverse heterocyclic frameworks biosynthetically derived from shikimate-terpene hybrids, but also exhibit intriguing bioactivities, such as antiviral activity and inhibition of protein tyrosine phosphatase 1B (PTP1B) and histamine release [5–10]. Our previous investigations on the *Rhododendron* plants revealed an array of optically pure meroterpenoid enantiomers that existed as naturally scalemic mixtures [5–7]. Some of these meroterpenoids have soon afterward aroused interests of synthetic chemists owing to their novel structures and promising bioactivities [11–13].

The plant *Rhododendron fastigiatum* Franch, mainly growing in Tibetan area, has not been chemically studied. In order to seek more structurally and biologically interesting meroterpenoids from the *Rhododendron* genus, research on the aerial parts of *R. fastigiatum* afforded five scalemic mixtures (**1**–**5**), together with grifolin (**6**) [14] and grifolinone A (**7**) [15]. Further chiral HPLC resolution of **1**–**5** provided five enantiomeric pairs of meroterpenoids, (+)-/(−)-fastinoids A–C (**1a/1b**, **2a/2b**, and **4a/4b**), (+)-/(−)-rubiginosin A (**3a/3b**), and (−)-/(+)-fastinoid D (**5a/5b**) (Fig. 1). Compounds **1a/1b**, **2a/2b**, **3b**, **4a/4b**, and **5a/5b** were new meroterpenoids incorporating diverse heterocyclic systems. Compounds **2a/2b**, **3a/3b**, **6**, and **7** showed PTP1B inhibitory activity *in vitro*. Herein, the isolation procedure, structural characterization, and biological evaluation of the isolates are reported.

Results and Discussion

Fastinoid A (**1**), an optically active substance ($[\alpha]_D^{25}$ +13.2), possessed the molecular formula $C_{22}H_{30}O_4$ based on the HRESI-MS (*m/z* 359.2221 $[M + H]^+$; Calcd. for $C_{22}H_{31}O_4$, 359.2222). The IR spectrum displayed the presence of hydroxy (3424 cm^{-1}), carbonyl (1659 cm^{-1}), and aromatic (1594 and 1472 cm^{-1}) functionalities. The 1D NMR and HSQC spectra exhibited signals (Tables 1 and 2) for a hydroxy group (δ_H 8.06, OH-5), a carbonyl carbon (δ_C 216.4, C-14), a 1, 2, 3,

[Received on] 16-Aug.-2019
[Research funding] This work was supported by the National Natural Science Foundation of China (No. 81222045) and the Fudan-SIMM Joint Research Fund (No. FU-SIMM20181011).
[*Corresponding author] Tel/Fax: 86-21-51980138, E-mails: chunlei@fudan.edu.cn (LEI Chun); ajhou@shmu.edu.cn (HOU Ai-Jun)
These authors have no conflict of interest to declare.
Dedicated to Professor SUN Han-Dong on the Occasion of His 80th Birthday

5-tetrasubstituted benzene ring (δ_H 6.36, H-6; 6.29, H-8; δ_C 107.7, C-4a; 155.6, C-5; 110.1, C-6; 138.5, C-7; 111.2, C-8; 154.6, C-8a), two oxygenated tertiary carbons (δ_C 83.1, C-2; 70.0, C-16), and a quaternary carbon (δ_C 41.5, C-12), together with resonances for five methyl singlets, four methylenes, and three methines. These data accounted for five indices of hydrogen deficiency (IHD), and the remaining ones required the existence of three additional rings. Therefore, **1** was supposed to have a tetracyclic framework including a benzene motif.

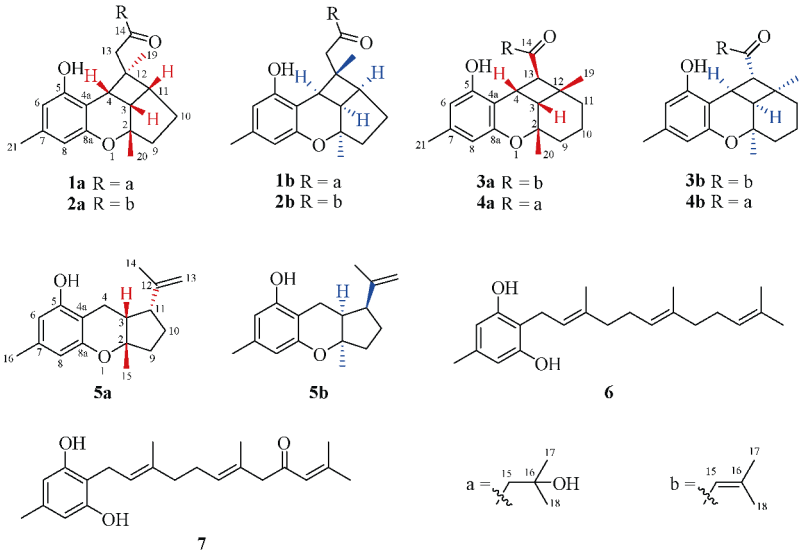

Fig. 1 Structures of the isolated compounds

Table 1 ^{1}H NMR data for compounds 1–5 in $CDCl_3$

Position	1 [a]	2 [b]	3 [a]	4 [a]	5 [b]
3	2.68, t (9.0)	2.68, t (8.8)	1.81, d (9.6)	1.81, d (9.0)	2.07, m
4	3.31, d (9.6)	3.38, d (10.0)	3.82, t (9.6)	3.85, t (9.6)	a 2.46, dd (13.6, 4.8)
					b 2.05, m
6	6.36, br s	6.39, br s	6.40, br s	6.40, br s	6.20, br s
8	6.29, br s	6.27, br s	6.30, br s	6.32, br s	6.29, br s
9	a 2.03, m	a 2.04, m	a 2.07, dt (13.8, 3.0)	a 2.08, dt (13.8, 3.6)	a 2.01, m
	b 1.55, m	b 1.54, m	b 1.35, m	b 1.34, td (13.8, 3.6)	b 1.76, m
10	a 1.76, m	a 1.76, m	a 1.97, m	a 1.96, m	a 1.96, m
	b 1.63, m	b 1.63, m	b 1.65, m	b 1.65, m	b 1.68, m
11	2.35, td (8.4, 2.4)	2.31, td (8.4, 2.4)	a 1.86, br d (13.8)	a 1.82, br d (13.8)	2.78, m
			b 1.30, td (13.8, 4.8)	b 1.31, td (13.8, 4.8)	
13	a 2.97, d (18.0)	a 2.97, d (17.6)	2.96, d (9.0)	2.98, d (9.6)	a 4.93, br s
	b 2.88, d (18.0)	b 2.79, d (17.6)			b 4.76, br s
14					1.77, s
15	a 2.71, d (16.8)	6.11, br s	5.87, br s	a 2.50, d (18.0)	1.42, s
	b 2.65, d (16.8)			b 2.45, d (18.0)	
16					2.21, s
17	1.29, s	1.93, br s	1.90, br s	1.25, s	
18	1.28, s	2.21, br s	2.16, br s	1.20, s	
19	0.84, s	0.84, s	1.15, s	1.20, s	
20	1.32, s	1.32, s	1.14, s	1.09, s	
21	2.23, s	2.23, s	2.23, s	2.23, s	
5-OH	8.06, s		7.49, s		

[a] Data were measured at 600 MHz; [b] Data were measured at 400 MHz

Table 2 ^{13}C NMR (150 MHz) data for compounds 1–5 in $CDCl_3$

Position	1	2	3	4	5
2	83.1	83.0	75.3	75.3	85.5
3	40.5	40.6	45.1	45.5	43.9
4	34.4	34.3	24.0	23.8	17.2
4a	107.7	108.0	112.1	111.6	108.0
5	155.6	156.2	153.4	152.9	153.1
6	110.1	110.4	110.6	110.6	108.3
7	138.5	138.2	138.0	138.4	137.1
8	111.2	110.8	111.5	112.0	110.8
8a	154.6	154.6	154.4	154.7	154.9
9	38.5	38.6	36.4	36.6	37.3
10	24.9	24.8	17.4	17.2	24.3
11	46.6	47.0	34.4	34.5	48.5
12	41.5	41.8	39.5	39.8	144.7
13	59.2	58.7	58.0	57.9	111.3
14	216.4	203.1	203.3	215.7	23.5
15	55.0	124.2	122.4	52.7	28.3
16	70.0	159.6	158.1	69.7	21.3
17	29.7	28.2	28.2	29.6	
18	29.5	21.5	21.5	29.5	
19	15.4	15.5	25.9	25.8	
20	26.3	26.3	29.7	29.4	
21	21.3	21.3	21.6	21.6	

The planar structure of **1** was constructed by detailed interpretation of its HMBC spectrum (Fig. 2). The HMBC correlations of H-4/C-2, C-3, C-4a, C-8a; H_3-20/C-2, C-3; OH-5/C-4a, C-5, C-6; and H_3-21/C-6, C-7, C-8 indicated a benzopyran moiety. The HMBC networks of H_3-20/C-9; H_2-9/C-2, C-10, C-11; H-4/C-12; H-11/C-3, C-10; and H_3-19/C-4, C-11, C-12 defined a cyclopentane unit and a cyclobutane motif. The HMBC cross-peaks of H_2-13/C-4, C-12, C-14, C-15, C-19 and H_2-15/C-14, C-16, C-17, C-18 indicated a 4-hydroxy-4-methylpent-2-one side chain at C-12. Thus, compound **1** was elucidated as a merosesquiterpene bearing the same benzo[*c*]-2-oxatricyclo[5.2.1.0^{5,10}]decane framework as rhodonoids E and F [6].

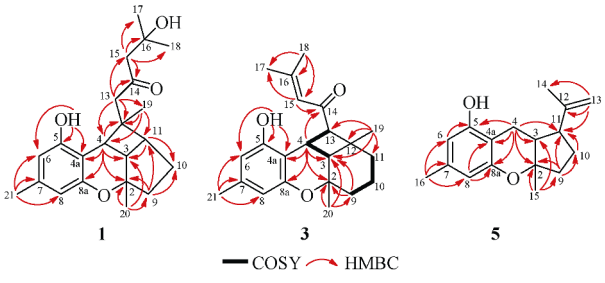

Fig. 2 ^{1}H-^{1}H COSY and key HMBC correlations for 1, 3, and 5

The H-3/H-4, H-11, H_3-20 NOESY correlations (Fig. 3) and the coupling constants of H-3/H-4 (J = 9.6 Hz) and H-3/H-11 (J = 8.4 Hz) [6–8] implied that H-3, H-4, H-11, and H_3-20 were cofacial, assigning a β-orientation for them. The NOESY correlations of H-9a/H_3-19 and H-9b/H_3-20 suggested an α-orientation for H_3-19. Chiral HPLC analysis showed that **1** was a scalemic mixture with an approximate ratio of 13 : 1 (Fig. 4). Two enantiomers with opposite specific rotations (**1a**: $[\alpha]_D^{25}$ +15.6; **1b**: $[\alpha]_D^{25}$ −15.2) and ECD curves (Fig. 4) were then obtained. A single-crystal X-ray diffraction study with Cu Kα radiation of **1a** determined its absolute configuration as (2*S*, 3*S*, 4*S*, 11*R*, 12*S*) [absolute configuration parameter: 0.07 (5)] (Fig. 5). As its enantiomer, the absolute configuration of **1b** was assigned as (2*R*, 3*R*, 4*R*, 11*S*, 12*R*). Compounds **1a** and **1b** were thereby structurally identified and named (+)-fastinoid A and (−)-fastinoid A, respectively.

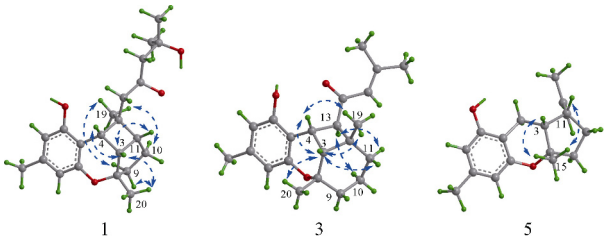

Fig. 3 Key NOESY correlations for 1, 3, and 5

Fastinoid B (**2**), $[\alpha]_D^{25}$ +6.7, was assigned the molecular formula $C_{22}H_{28}O_3$ by HRESI-MS (*m/z* 341.2118 [M + H]$^+$; Calcd. for $C_{22}H_{29}O_3$, 341.2117). Its NMR data (Tables 1 and 2) resembled those of **1** except signals attributable to a 4-methylpent-3-en-2-one moiety at C-12 in **2** rather than the 4-hydroxy-4-methylpent-2-one group in **1**, which could be deduced from the HMBC correlations of H_2-13/C-4, C-12, C-14, C-19 and H-15/C-14, C-17, C-18. The relative configuration of **2** was identical to that of **1** based on their NMR data comparison and the NOESY experiment. This compound is a new natural product, which has been synthetized as a racemate [11]. Two enantiomers (**2a**: $[\alpha]_D^{25}$ +16.5; **2b**: $[\alpha]_D^{25}$ −16.3) with a ratio of approximately 2 : 1 were separated from **2** by chiral HPLC (Fig. 4). Comparison of the ECD spectra of **1a**/**1b** and **2a**/**2b** revealed that the two enantiomeric pairs displayed similar Cotton effects (Fig. 4). Thus, the absolute configurations were identified as (2*S*, 3*S*, 4*S*, 11*R*, 12*S*) for **2a** and (2*R*, 3*R*, 4*R*, 11*S*, 12*R*) for **2b**. Compounds **2a**/**2b** are new meroterpenoids and named (+)-fastinoid B (**2a**) and (−)-fastinoid B (**2b**), respectively.

Compound **3** had a specific rotation of $[\alpha]_D^{25}$ +32.0. Its molecular formula was established as $C_{22}H_{28}O_3$ by the HRESI-MS (*m/z* 341.2112 [M + H]$^+$; Calcd. for $C_{22}H_{29}O_3$, 341.2117). The ^{1}H and ^{13}C NMR spectra (Tables 1 and 2) with DEPT and HSQC experiments differentiated the existence of a hydroxy group, a carbonyl carbon, a 1, 2, 3, 5-tetrasubstituted

benzene moiety, a trisubstituted double bond, five methyl singlets, three methylenes, three methines, an oxygenated tertiary carbon, and a quaternary carbon. In consideration of nine IHDs, three additional rings should be present in **3**. The planar structure of **3** was assembled by its 2D NMR data (Fig. 2). The ^{1}H-^{1}H COSY and HSQC spectra provided two structural fragments of CH(3)–CH(4)–CH(13) and CH_2(9)–CH_2(10)–CH_2(11). The HMBC cross-peaks of H-4/C-2, C-3, C-4a, C-8a; OH-5/C-4a, C-5, C-6; H-9/C-2, C-3; H_3-19/C-3, C-11, C-12, C-13; H_3-20/C-2, C-3, C-9; and H_3-21/C-6, C-7, C-8 verified that **3** had the same benzo[*c*]-2-oxatricyclo[5.3.1.0^{5,11}]undecane ring system as rhodonoid A [5]. The HMBC correlations of H-4/C-14; H-15/C-14, C-17, C-18; and H_3-18/C-15, C-16, C-17 indicated a 3-methylbut-2-en-1-one moiety at C-13.

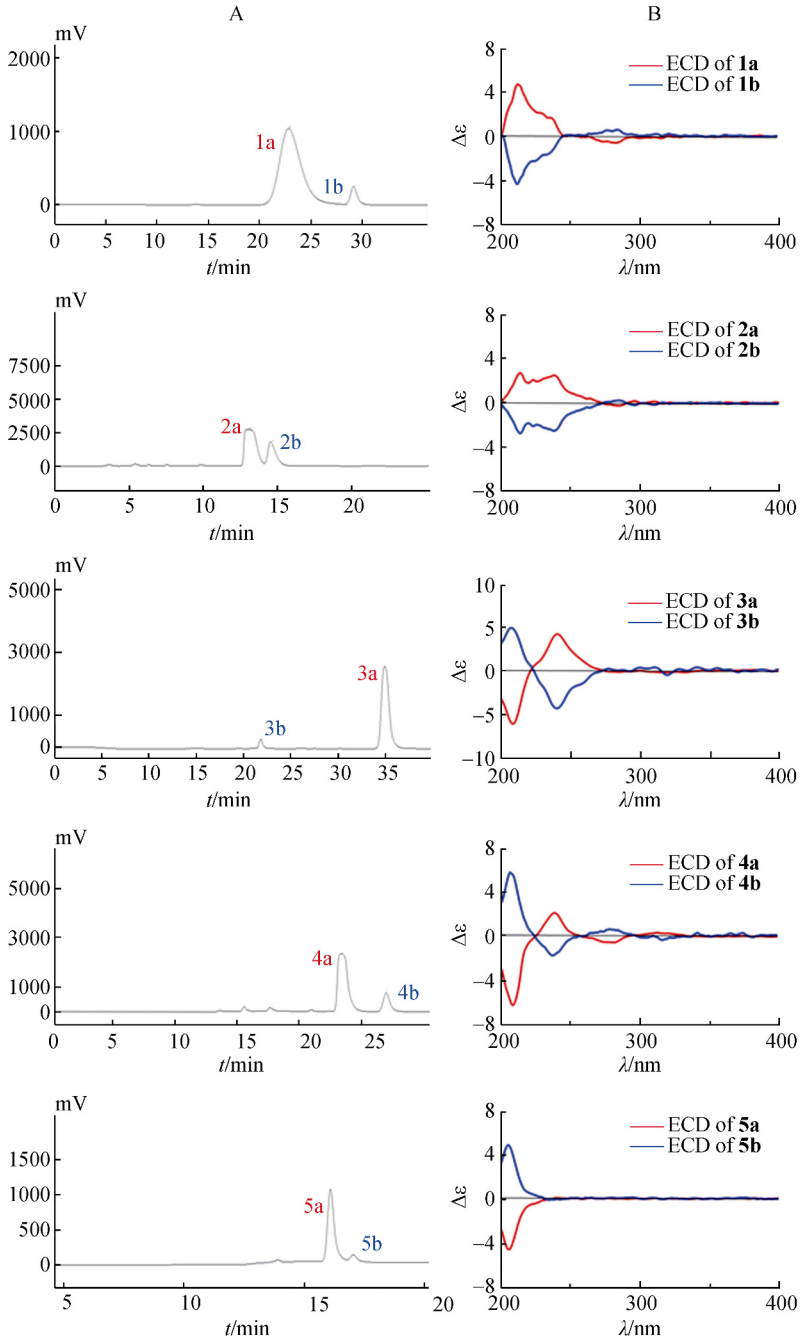

Fig. 4 Chiral separation chromatograms (A) and ECD spectra (B) for enantiomers 1a/1b–5a/5b

The relative configuration of compound **3** was proposed by analyzing the NOESY interactions (Fig. 3). The key NOESY correlations of H-3/H-4, H-11b, H_3-19, H_3-20; H-4/H_3-19 indicated that these protons were cofacial and *β*-oriented. Subsequently, the observed NOESY cross-peaks of H-13/H-11a suggested that they were *α*-oriented. Chiral-phase resolution of **3**, a scalemic mixture with an approximate ratio of 15 : 1, yielded enantiomers **3a** ($[\alpha]_D^{25}$ +36.7) and **3b**

($[\alpha]_D^{25}$ −36.0) (Fig. 4). A single crystal of **3a** was obtained, and an X-ray crystallographic analysis with Cu Kα radiation was carried out (Fig. 5). The Flack parameter for **3a** is 0.0(3), allowing an explicit assignment of the absolute configuration as (2*S*, 3*R*, 4*S*, 12*R*, 13*R*). Meanwhile, the absolute configuration of **3b** was defined as (2*R*, 3*S*, 4*R*, 12*S*, 13*S*). Compound **3a** was previously isolated from *R. rubiginosum* as rubiginosin A [16]. Compound **3b** is a new meroterpenoid and named (−)-rubiginosin A.

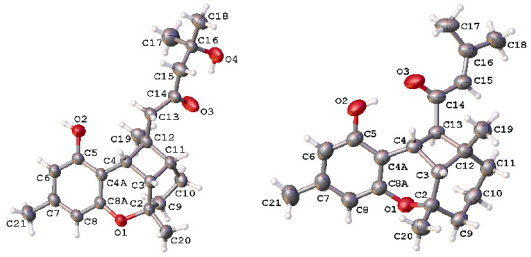

Fig. 5 X-ray ORTEP plots for 1a and 3a

Fastinoid C (**4**) was elucidated to be an analogue of **3**, as suggested by the HRESI-MS and NMR data (Tables 1 and 2). Further examination of the NMR data revealed the replacement of the 3-methylbut-2-en-1-one unit in **3** by a 3-hydroxy-3-methylbutan-1-one group at C-13 in **4**, as judged by the HMBC correlations of H-4/C-13, C-14 and H-15/C-14, C-16, C-17, C-18. The relative configuration of **4** was the same as that of **3**, as confirmed by the identical NOESY data. Compound **4** was also a scalemic mixture ($[\alpha]_D^{25}$ +7.3) with the approximate ratio 4 : 1 (Fig. 4). By chiral-phase resolution, two enantiomers (**4a**: $[\alpha]_D^{25}$ +13.5; **4b**: $[\alpha]_D^{25}$ −13.4) with similar ECD curves to those of **3a**/**3b** were obtained (Fig. 4). Thus, the absolute configurations of **4a** and **4b** were assigned as (2*S*, 3*R*, 4*S*, 12*R*, 13*R*) and (2*R*, 3*S*, 4*R*, 12*S,* 13*S*), respectively. Enantiomers **4a** and **4b** were structurally identified and named (+)-fastinoid C and (−)-fastinoid C, respectively.

Fastinoid D (**5**), $[\alpha]_D^{25}$ −7.0, gave a $[M + H]^+$ ion at *m/z* 259.1695 (Calcd. 259.1698) in the HRESI-MS, corresponding to the molecular formula $C_{17}H_{22}O_2$. Its NMR data (Tables 1 and 2) and HMBC correlations (Fig. 2) revealed that **5** possessed the same benzo[*c*]-2-oxadicyclo[4.3.0]nonane scaffold as nyingchinoid C [7]. The structural difference resulted from the 1, 2, 3, 5-tetrasubstituted benzene ring. The HMBC correlations of H_3-16/C-6, C-7, C-8; H-8/C-4a, C-8a; and H_2-4, H-6/C-5 assigned the aromatic methyl at C-7 and the hydroxyl at C-5 (Fig. 2). The relative configuration was identical to that of nyingchinoid C. The NOESY correlations of H_3-15 with both H-3 and H-11 indicated a β-orientation for these protons (Fig. 3). The chiral HPLC resolution for **5** showed the existence of a scalemic mixture (3 : 1) and afforded two enantiomers (**5a**: $[\alpha]_D^{25}$ −10.2; **5b**: $[\alpha]_D^{25}$ +9.3) (Fig. 4). The ECD spectra of **5a** and **5b** (Fig. 4) respectively matched well with those of (−)-nyingchinoid C (2*S*, 3*R*, 11*R*) and (+)-nyingchinoid C (2*R*, 3*S*, 11*S*) [7]. Thus, the absolute configurations were elucidated as (2*S*, 3*R*, 11*R*) for **5a** and (2*R*, 3*S*, 11*S*) for **5b**, and the compounds were named (−)-fastinoid D and (+)-fastinoid D, respectively.

Two known compounds, grifolin (**6**) [14] and grifolinone A (**7**) [15], were isolated and identified.

Compounds **1a**/**1b**–**5a**/**5b** and **7** were evaluated for their inhibitory effects on PTP1B *in vitro*, and oleanolic acid [17–18] was used as positive control (IC_{50} 8.4 ± 0.1 μmol·L^{-1}). Compounds **2a**/**2b**, **3a**/**3b**, and **7** exhibited inhibitory effects with IC_{50} values of 47.0 ± 1.7 (**2a**), 54.9 ± 9.7 (**2b**), 40.9 ± 2.6 (**3a**), 49.2 ± 1.4 (**3b**), and 13.0 ± 1.4 (**7**) μmol·L^{-1}, respectively. Compound **6** is also active and its IC_{50} value (5.7 ± 0.5 μmol·L^{-1}) has been reported recently by our group [7].

Experimental

General experimental procedures

Melting points were recorded on a SGM X-4 apparatus. Optical rotations were measured on a Rudolph Autopol IV polarimeter (Rudolph Research Analytical, NJ, USA). UV and ECD spectra were obtained on a JASCO J-810 instrument (JASCO International Co., Ltd., Tokyo, Japan). IR spectra were measured on a Nicolet iS5 spectrometer (Thermo Fisher Scientific, MA, USA). NMR spectra were obtained on a Varian Mercucy Plus 400 MHz (Varian Medical Systems Inc., CA, USA) and a Bruker Avance 600 MHz spectrometers (Bruker Biospin GmbH, Rheinstetten, Germany) with $CDCl_3$ as solvent. HRESI-MS data were obtained on an AB 5600+ (AB SCIEX LLC., MA, USA) or a Waters-Micromass Q-TOF mass spectrometer (Waters Corporation, MA, USA). Diaion HP-20 (Mitsubishi Chemical Co., Japan), silica gel (200–300 mesh, Qingdao Haiyang Chemical Co., Ltd., China), and ODS gel (50 μm, YMC Co., Kyoto, Japan) were used for column chromatography (CC). Precoated silica gel GF254 plates (Qingdao Haiyang Chemical Co., Ltd., China) were used for TLC. Semi-preparative HPLC and chiral-phased separation were carried out on a Shimadzu Essentia LC-16 with a UV detector (210 and 254 nm), using a YMC C_{18} column (150 mm × 10 mm, 5 μm, YMC Co., Kyoto, Japan), a Daicel chiralpak IC column [250 mm × 20 mm, 5 μm, Daicel Chiral Technologies (China) Co., Ltd.], or a Daicel chiralpak IF column [250 mm × 10 mm, 5 μm, Daicel Chiral Technologies (China) Co., Ltd.], respectively.

Plant material

The aerial parts of *R. fastigiatum* were collected in Shangri-La County of Yunnan Province, China, in June 2009. The plant material was identified by Dr. LI Xin-Hui, Kunming Institute of Botany, Chinese Academy of Sciences. A voucher specimen (TCM 09-06-03 Hou) has been deposited at the Herbarium of the Department of Pharmacognosy, School of Pharmacy, Fudan University.

Extraction and isolation

The air-dried plant material (7 kg) was ground and extracted with 95% EtOH at room temperature. After evaporation under reduced pressure, a crude extract (1.2 kg) was obtained and partitioned between EtOAc and H_2O. The EtOAc extract (450 g) was isolated by Diaion HP-20 CC (EtOH−H_2O, 1 : 9, 3 : 7, 6 : 4, 9 : 1, *V/V*) to provide fractions A–D. Fraction C (130 g) was chromatographed on a silica gel column

(petroleum ether−EtOAc, 50 : 1, 25 : 1, 12 : 1, 6 : 1, 3 : 1, 2 : 1, *V/V*) to give fractions C1–C8. Fraction C2 (12.0 g) was subjected to silica gel CC (petroleum ether−acetone, 40 : 1, 20 : 1, 10 : 1, 1 : 1, *V/V*) to yield fractions C2a–C2d. Fraction C2b (1.5 g) was isolated by ODS gel CC (MeOH−H_2O, 7 : 3, 8 : 2, 9 : 1, *V/V*), followed by semi-preparative HPLC (MeOH−H_2O, 7 : 3) to afford **2** (8.0 mg) and **5** (7.0 mg). Fractions C6 (20.0 g) and C7 (16.0 g) were separated by silica gel CC (petroleum ether−acetone, 20 : 1, 10 : 1, 5 : 1, 1 : 1, *V/V*) to produce fractions C6a–C6d and C7a–C7d, respectively. Fraction C6b (4.3 g) was isolated by ODS gel CC (MeOH−H_2O, 7 : 3, 8 : 2, 9 : 1, *V/V*) and then by HPLC (MeOH−H_2O, 6.5 : 3.5, *V/V*) to afford **4** (15.0 mg) and **7** (12.0 mg). Using the same procedure as fraction C2b, fraction C6c (3.5 g) gave **1** (7.0 mg) and **6** (15.0mg) and fraction C7b (3.2 g) provided **3** (15.0 mg).

Chiral resolution

Compounds **1–5** were subjected to chiral-phase HPLC resolution (Fig. 4) eluted by *n*-hexane−isopropanol (7.5 : 2.5 for **1**, 9.3 : 0.7 for **2**, 8 : 2 for **3** and **4**, and 8.5 : 1.5 for **5**) with a flow rate of 4.0 mL·min^{-1}. A Daicel chiralpak IC column was used for **1** and **3–5** and an IF column for **2**. The UV wavelength was set at 210 nm and the temperature was 20 °C. The peak area ratios were 13 : 1 (**1a** : **1b**), 2 : 1 (**2a** : **2b**), 15 : 1 (**3a** : **3b**), 4 : 1 (**4a** : **4b**), and 3 : 1 (**5a** : **5b**). Five pairs of enantiomers were acquired, including **1a** (2.3 mg)/**1b** (0.8 mg), **2a** (3.7 mg)/**2b** (1.2 mg), **3a** (6.9 mg)/**3b** (1.7 mg), **4a** (5.7 mg)/**4b** (1.0 mg), and **5a** (2.2 mg)/**5b** (0.8 mg).

Fastinoid A (**1**): White amorphous powder; $[\alpha]_D^{25}$ +13.2 (*c* 0.1, MeOH); UV (MeOH) λ_{max} (log ε) 212 (4.38), 235 (3.81), 283 (3.09) nm; IR (KBr) ν_{max}: 3424, 2925, 2853, 1659, 1594, 1472, 1415, 1312, 1198, 1178, 1135, 1078, 1033, 976 cm^{-1}; ^{1}H and ^{13}C NMR data, see Tables 1 and 2; positive HRESI-MS *m/z* 359.2221 $[M + H]^+$ (Calcd. for $C_{22}H_{31}O_4$, 359.2222).

(+)-Fastinoid A (**1a**): Colorless crystals (MeOH): 166–168 °C; $[\alpha]_D^{25}$ +15.6 (*c* 0.1, MeOH); ECD (MeOH) λ_{max} nm ($\Delta\varepsilon$) 212 (+4.98), 237 (+1.52), 284 (–0.54).

(−)-Fastinoid A (**1b**): White amorphous powder; $[\alpha]_D^{25}$ −15.2 (*c* 0.1, MeOH); ECD (MeOH) λ_{max} nm ($\Delta\varepsilon$) 211 (–4.58), 236 (–1.48), 283 (+0.60).

Fastinoid B (**2**): White amorphous powder; $[\alpha]_D^{25}$ +6.7 (*c* 0.2, MeOH); UV (MeOH) λ_{max} (log ε) 211 (4.28), 236 (3.98), 282 (3.04) nm; IR (KBr) ν_{max}: 3377, 2925, 2856, 1679, 1614, 1452, 1377, 1195, 1180, 1135, 1073, 1048, 1023, 973 cm^{-1}; ^{1}H and ^{13}C NMR data, see Tables 1 and 2; positive HRESI-MS *m/z* 341.2118 $[M + H]^+$ (Calcd. for $C_{22}H_{29}O_3$, 341.2117).

(+)-Fastinoid B (**2a**): White amorphous powder; $[\alpha]_D^{25}$ +16.5 (*c* 0.1, MeOH); ECD (MeOH) λ_{max} nm ($\Delta\varepsilon$) 212 (+3.13), 238 (+2.57), 285 (–0.22).

(−)-Fastinoid B (**2b**): White amorphous powder; $[\alpha]_D^{25}$ −16.3 (*c* 0.1, MeOH); ECD (MeOH) λ_{max} nm ($\Delta\varepsilon$) 212 (–3.12), 238 (–2.52), 285 (+0.20).

Rubiginosin A (**3**): White amorphous powder; $[\alpha]_D^{25}$ +32.0 (*c* 0.1, MeOH); UV (MeOH) λ_{max} (log ε) 208 (3.97), 238 (3.59), 283 (3.01) nm; IR (KBr) ν_{max}: 3419, 2925, 2848, 1657, 1602, 1470, 1315, 1200, 1183, 1133, 1078, 1043, 978 cm^{-1}; ^{1}H and ^{13}C NMR data, see Tables 1 and 2; positive HRESI-MS *m/z* 341.2112 $[M + H]^+$ (Calcd. for $C_{22}H_{29}O_3$, 341.2117).

(+)-Rubiginosin A (**3a**): Colorless crystals (MeOH): 161−162 °C; $[\alpha]_D^{25}$ +36.7 (*c* 0.1, MeOH); ECD (MeOH) λ_{max} nm ($\Delta\varepsilon$) 208 (–5.90), 240 (+4.20), 282 (–0.20).

(−)-Rubiginosin A (**3b**): White amorphous powder (MeOH); $[\alpha]_D^{25}$ −36.0 (*c* 0.1, MeOH); ECD (MeOH) λ_{max} nm ($\Delta\varepsilon$) 208 (+5.10), 241 (–4.20), 282 (+0.10).

Fastinoid C (**4**): White amorphous powder; $[\alpha]_D^{25}$ +7.3 (*c* 0.1, MeOH); UV (MeOH) λ_{max} (log ε) 209 (4.51), 232 (3.80), 280 (3.12) nm; IR (KBr) ν_{max}: 3414, 2925, 2853, 1659, 1592, 1462, 1425, 1320, 1198, 1180, 1135, 1073, 1046, 978 cm^{-1}; ^{1}H and ^{13}C NMR data, see Tables 1 and 2; positive HRESI-MS *m/z* 359.2210 $[M + H]^+$ (Calcd. for $C_{22}H_{31}O_4$, 359.2222).

(+)-Fastinoid C (**4a**): White amorphous powder; $[\alpha]_D^{25}$ +13.5 (*c* 0.1, MeOH); ECD (MeOH) λ_{max} nm ($\Delta\varepsilon$) 209 (–6.00), 238 (+2.10), 280 (–0.52).

(−)-Fastinoid C (**4b**): White amorphous powder; $[\alpha]_D^{25}$ −13.4 (*c* 0.1, MeOH); ECD (MeOH) λ_{max} nm ($\Delta\varepsilon$) 208 (+5.70), 236 (–2.00), 282 (+0.56).

Fastinoid D (**5**): White amorphous powder; $[\alpha]_D^{25}$ −7.0 (*c* 0.1, MeOH); UV (MeOH) λ_{max} (log ε) 208 (3.90), 232 (3.23) nm; IR (KBr) ν_{max} : 3402, 2928, 2856, 1617, 1597, 1517, 1452, 1195, 1183, 1136, 1076, 1043 cm^{-1}; ^{1}H and ^{13}C NMR data, see Tables 1 and 2; positive HR-ESI-MS *m/z* 259.1695 $[M + H]^+$ (Calcd. for $C_{17}H_{23}O_2$, 259.1698).

(−)-Fastinoid D (**5a**): White amorphous powder; $[\alpha]_D^{25}$ −10.2 (*c* 0.1, MeOH); ECD (MeOH) λ_{max} nm ($\Delta\varepsilon$) 206 (–4.65).

(+)-Fastinoid D (**5b**): White amorphous powder; $[\alpha]_D^{25}$ +9.3 (*c* 0.1, MeOH); ECD (MeOH) λ_{max} nm ($\Delta\varepsilon$) 205 (+4.70).

X-ray crystallographic analysis

The crystals of **1a** were obtained from MeOH−H_2O (9 : 1), and those of **3a** from MeOH. Single-crystal X-ray diffraction experiments were performed on a Bruker APEX-II CCD detector (Bruker AXS GmbH, Karlsruhe, Germany) using graphite-monochromated Cu Kα radiation (λ = 1.54178 Å). The structure of **1a** was solved by direct methods using the SHELXS-97 program (Sheldrick 2008) [19] and refined with full-matrix least-squares calculations on F^2 using the SHELXL-2013 package (Sheldrick 2013) [20], and that of **3a** was solved by the SHELXT structure solution program (Sheldrick 2015) [21] and the SHELXL refinement package (Sheldrick 2015) [22]. Their crystallographic data have been deposited at the Cambridge Crystallographic Data Center (deposition No. CCDC 1845682 for **1a** and CCDC 1845692 for **3a**). Copy of the data can be obtained free of charge on application to CCDC, 12 Union Road, Cambridge CB2 1EZ, UK [fax: Int. +44(0)(1223) 336-033]; E-mail: deposit@ccdc. cam.ac.uk].

Crystal data for (+)-fastinoid A (**1a**): $C_{22}H_{32}O_5$, M = 376.47, *a* = 9.1203(3) Å, *b* = 9.9702(3) Å, *c* = 22.6622(7) Å; α = 90°, β = 90°, γ = 90°, *V* = 2060.70(11) Å^3, *T* = 296(2) K,

space group *P*21 21 21, Z = 4, μ(Cu Ka) = 0.683 mm^{-1}; 33346 reflections collected, 3653 independent reflections (R_{int} = 0.0532); the final R_1 values were 0.0419 [$I > 2\sigma(I)$]; the final $wR(F^2)$ values were 0.1218 [$I > 2\sigma(I)$]; the final R_1 values were 0.0426 (all data); the final $wR(F^2)$ values were 0.1229 (all data); the goodness of fit on F^2 was 1.045; flack parameter = 0.07 (5).

Crystal data for (+)-rubiginosin A (**3a**): $C_{22}H_{28}O_3$, M = 340.44, a = 18.1156(4) Å, b = 9.0393(3) Å, c = 12.0808(3) Å; α = 90°, β = 103.956(2)°, γ = 90°, V = 1919.86(9) $Å^3$, T = 296 K, space group C 1 2 1, Z = 4, μ(Cu Ka) = 0.606 mm^{-1}; 6527 reflections collected, 2749 independent reflections (R_{int} = 0.0526); the final R_1 values were 0.0505 [$I > 2\sigma(I)$]; the final $wR(F^2)$ values were 0.1497 [$I > 2\sigma(I)$]; the final R_1 values were 0.0551 (all data); the final $wR(F^2)$ values were 0.1572 (all data); the goodness of fit on F^2 was 1.036; flack parameter = 0.0 (3).

Assay of PTP1B activity

The PTP1B activity assay was carried out according to the procedure described previously [23–24]. Oleanolic acid and DMSO were used as the positive and negative controls, respectively. The result of PTP1B inhibition was expressed as IC_{50}, which was calculated with Prism 4 software (Graphpad, San Diego, CA).

References

[1] Fang MY, Fang RZ, He MY, *et al*. *Flora of China* [M]. Beijing: Science Press, 2005, 14: 260-455.

[2] Li Y, Liu YB, Zhang JJ, *et al*. Antinociceptive grayanoids from the roots of *Rhododendron molle* [J]. *J Nat Prod*, 2015, **77**(12): 2887-2895.

[3] Zhou J, Zhan G, Zhang H, *et al*. Rhodomollanol A, a highly oxygenated diterpenoid with a 5/7/5/5 tetracyclic carbon skeleton from the leaves of *Rhododendron molle* [J]. *Org Lett*, 2017, **19**(14): 3935-3938.

[4] Zhou J, Liu T, Zhang H, *et al*. Anti-inflammatory grayanane diterpenoids from the leaves of *Rhododendron molle* [J]. *J Nat Prod*, 2018, **81**(1): 151-161.

[5] Liao HB, Lei C, Gao LX, *et al*. Two enantiomeric pairs of meroterpenoids from *Rhododendron capitatum* [J]. *Org Lett*, 2015, **17**(20): 5040-5043.

[6] Liao HB, Huang GH, Yu MH, *et al*. Five pairs of meroterpenoid enantiomers from *Rhododendron capitatum* [J]. *J Org Chem*, 2017, **82**(3): 1632-1637.

[7] Huang GH, Hu Z, Lei C, *et al*. Enantiomeric pairs of meroterpenoids with diverse heterocyclic systems from *Rhododendron nyingchiense* [J]. *J Nat Prod*, 2018, **81**(8): 1810-1818.

[8] Kashiwada Y, Yamazak K, Ikeshiro Y, *et al*. Isolation of rhododaurichromanic acid B and the anti-HIV principles rhododaurichromanic acid A and rhododaurichromenic acid from *Rhododendron dauricum* [J]. *Tetrahedron*, 2001, **57**(8): 1559-1563.

[9] Iwata N, Kitanaka S. Tetracyclic chromane derivatives from *Rhododendron anthopogonoides* [J]. *J Nat Prod*, 2010, **73**(7): 1203-1206.

[10] Seephonkai P, Popescu R, Zehl M, *et al*. Ferruginenes A–C from *Rhododendron ferrugineum* and their cytotoxic evaluation [J]. *J Nat Prod*, 2011, **74**(4): 712-717.

[11] Wu H, Hsung RP, Tang Y. Total syntheses of (±)-rhodonoids A and B and C12-*epi*-rhodonoid B [J]. *J Org Chem*, 2017, **82**(3): 1545-1551.

[12] Wu H, Hsung RP, Tang Y. Total syntheses of (±)-rhodonoids C, D, E, F, and G and ranhuadujuanine B [J]. *Org Lett*, 2017, **19**(13): 3505-3507.

[13] Day AJ, Lam HC, Sumby CJ, *et al*. Biomimetic total synthesis of rhodonoids C and D, and murrayakonine D [J]. *Org Lett*, 2017, **19**(10): 2463-2465.

[14] Nukata M, Hashimoto T, Yamamoto I, *et al*. Neogrifolin derivatives possessing anti-oxidative activity from the mushroom *Albatrellus ovinus* [J]. *Phytochemistry*, 2002, **59**(7): 731-737.

[15] Quang DN, Hashimoto T, Arakawa Y, *et al*. Grifolin derivatives from *Albatrellus caeruleoporus*, new inhibitors of nitric oxide production in RAW 264.7 cells [J]. *Bioorg Med Chem*, 2006, **14**(1): 164-168.

[16] Yang YX, Wang JX, Wang Q, *et al*. New chromane and chromene meroterpenoids from flowers of *Rhododendron rubiginosum* Franch. *var*. *rubiginosum* [J]. *Fitoterapia*, 2018, **127**: 396-401.

[17] Liang LF, Kurtán T, Mándi A, *et al*. Unprecedented diterpenoids as a PTP1B inhibitor from the hainan soft coral *Sarcophyton trocheliophorum* Marenzeller [J]. *Org Lett*, 2013, **15**(2): 274-277.

[18] Lee JS, Abdjul DB, Yamazaki H, *et al*. Strongylophorines, new protein tyrosine phosphatase 1B inhibitors, from the marine sponge *Strongylophora strongilata* collected at Iriomote Island [J]. *Bioorg Med Chem Lett*, 2015, **25**(18): 3900-3902.

[19] Sheldrick GM. A Short history of SHELX [J]. *Acta Cryst A*, 2008, **64**: 112-122.

[20] Sheldrick GM. Recent developments in SHELX [J]. *Acta Cryst A*, 2013, **69**: S74.

[21] Sheldrick GM. SHELXT-integrated space-group and crystal-structure determination [J]. *Acta Cryst A*, 2015, **71**: 3-8.

[22] Sheldrick GM. Crystal structure refinement with SHELXL [J]. *Acta Cryst C*, 2015, **71**: 3-8.

[23] Shi L, Yu HP, Zhou YY, *et al*. Discovery of a novel competitive inhibitor of PTP1B by high-throughput screening [J]. *Acta Pharmacol Sin*, 2008, **29**(2): 278-284.

[24] Wang M, Yu BW, Yu MH, *et al*. New isoprenylated phenolic compounds from *Morus laevigata* [J]. *Chem Biodiversity*, 2015, **12**(6): 937-945.

Cite this article as: HUANG Guang-Hui, LEI Chun, ZHU Ke-Xin, LI Jing-Ya, LI Jia, HOU Ai-Jun. Enantiomeric pairs of meroterpenoids from *Rhododendron fastigiatum* [J]. *Chin J Nat Med*, 2019, **17**(12): 963-969.

Prof. HOU Ai-Jun, Ph.D, Fudan Universtity

Dr. HOU is currently a Professor at School of Pharmacy, Fudan University. Her research interests focus on drug discovery and development from TCM, with cancer and diabetes as particular targets. She has published over 100 research papers and 14 patents have been authorized. She has obtained excellent young scientist fund of the National Natural Science Foundation of China and New Century Excellent Talents award of the Ministry of Education, and has been awarded the Shanghai Shu Guang Scholar by Shanghai Municipal Education Commission.